Graphene/epoxy coating with radiation heat dissipation properties for spacecraft thermal management

Ning Li, Zhang Yibo, Yawei Xu, Jing Li

PII: S1385-8947(25)05941-8

DOI: https://doi.org/10.1016/j.cej.2025.165105

Reference: CEJ 165105

To appear in:

Received date: 30 March 2025

Revised date: 28 May 2025

Accepted date: 18 June 2025

Please cite this article as: N. Li, Z. Yibo, Y. Xu, et al., Graphene/epoxy coating with radiation heat dissipation properties for spacecraft thermal management, (2024), https://doi.org/10.1016/j.cej.2025.165105

Graphene/Epoxy Coating with Radiation Heat Dissipation properties for Spacecraft Thermal Management

Ning Li [1], Zhang Yibo[1], Yawei Xu [2], Jing Li [1, 3, **]*

1 School of Chemistry and Chemical Engineering, South China University of Technology, Guangzhou 510641, P. R. China

2 National Key Laboratory of Spacecraft Thermal Control, Beijing Institute of Spacecraft System Engineering, Beijing 100086, P. R. China

3 South China University of Technology-Zhuhai Institute of Modern Industrial Innovation, Zhuhai 519000, P. R. China

* Corresponding Authors: 18792530289@163.com

** Corresponding Authors: ljing@scut.edu.cn

Abstract: In the space environment, the heat dissipation of spacecraft primarily relies on thermal radiation. To reduce the weight of spacecraft, it is necessary to replace the existing copper radiators with aluminum ones. However, aluminum radiators have a lower emissivity, which results in suboptimal heat dissipation performance. Therefore, enhancing the emissivity of aluminum radiators is crucial for improving their heat dissipation performance. This study investigates the rapid (100 s) reduction of graphene oxide (GO) into low-defect reduced graphene oxide (mRGO) using Joule heating for 100

seconds, followed by non-covalent modification to further enhance its dispersion in water. By incorporating modified reduced graphene oxide (mRGO) as the primary filler in an aqueous epoxy resin emulsion and using 3-aminopropyltriethoxysilane (APTES) to enhance the adhesion between the coating and the aluminum substrate, a composite Graphene/Epoxy radiation heat dissipation coating (GERC) with high emissivity and strong adhesion was successfully prepared. Experimental results demonstrate that the coating containing 4 wt% mRGO filler exhibits the optimal heat dissipation efficiency (24.15%) and significantly enhances the infrared emissivity of the substrate (up to 0.93). This coating exhibits excellent thermal stability and strong adhesion, providing a novel approach for thermal management in space radiators.

Keywords：Joule heat, Reduced graphene oxide, Non-covalent modification, Silane coupling agent, Aluminum Radiator, Radiation heat dissipation coating

1 Introduction

In the space environment, the available space and power for spacecraft are limited, making traditional active cooling methods, such as forced convection and liquid circulation cooling, often inadequate to meet heat dissipation demands.[1-2] Traditional radiators used in spacecraft primarily include flat-plate radiators and heat pipe radiators. Flat-plate radiators are simple and reliable, utilizing the Stefan-Boltzmann law to dissipate heat through their surface area.[3] However, their fixed area limits scalability, making it difficult to meet the increasing heat dissipation demands of modern spacecraft. Heat pipe radiators, on the other hand, employ phase-change fluids (e.g., ammonia) to efficiently transfer heat to radiating surfaces.[4] While they offer flexibility and lightweight designs suitable for satellites, their performance is limited by the temperature range of the working fluid. Despite their widespread use, traditional aluminum radiators suffer from low surface emissivity (typically 0.1–0.2), which significantly restricts their ability to dissipate heat through radiation.[6] This limitation becomes particularly problematic in scenarios requiring high-efficiency heat dissipation, such as those encountered in spacecraft with limited space and power resources.[7] As a result, there is a pressing need to enhance the radiative performance of aluminum radiators to improve their overall heat dissipation efficiency.

To enhance the thermal efficiency of aluminum radiators, recent research has explored

surface treatments to increase emissivity. For example, elevating the emissivity of aluminum to ~0.9 can boost radiative contribution to approximately 30–40% of total heat dissipation.[8] Hadi et al. employed chemical spraying to deposit graphene layers of varying thicknesses on aluminum surfaces, demonstrating through wind tunnel tests that coated radiators achieved higher thermal efficiency than uncoated counterparts, peaking at an optimal thickness.[9] Zu et al. developed a carbon-nano-SiO_2 composite coating with an emissivity of 0.934, reducing equilibrium temperatures effectively.[10] Lee et al. reported self-assembled multi-walled carbon nanotube (MWCNT)-polyethyleneimine (PEI) coatings, enhancing heat dissipation by 19% and reducing thermal resistance by 16% compared to bare aluminum.[11] Despite these advances, a critical research gap persists coating adhesion under thermal cycling. In spacecraft applications, the temperature of heat dissipation components fluctuates frequently due to changes in orbital position. The significant difference in the coefficients of thermal expansion between the coating and the aluminum substrate can lead to insufficient adhesion, causing the coating to peel off and fail, which severely impacts the lifespan and performance of the thermal coatings.[16] Current studies, however, have largely overlooked adhesion, limiting the practical deployment of these coatings in space.

Wang et al. used γ-glycidoxypropyltrimethoxysilane (KH560) to treat sandblasted aluminum plates through salinization, successfully preparing polyamide 6-alumina composite joints with high bonding strength.[17] The study showed that after treatment with

a 10 wt% silane solution, the bonding strength of the joints increased significantly by 182%, reaching 37.8 MPa, and the strength remained at 60% even after high-temperature annealing. Lee et al. significantly enhanced the bonding strength of aluminum by forming a self-assembled monolayer on the aluminum surface using (3-mercaptopropyl) trimethoxysilane (MPTMS), which played a crucial role in the development of high-performance aluminum vibration damping plates (VDP).[18] The study found that after treating the aluminum surface with a 2% MPTMS solution for 7 minutes at high temperature, the surface was completely covered by a self-assembled monolayer, and the peel strength of the VDP increased by 180% compared to untreated samples, while damping properties were also enhanced. The use of silane coupling agents can effectively enhance the adhesion of coatings on aluminum substrates.

This study introduces a method for rapidly reducing graphene oxide (GO) via Joule heating. Reduced graphene oxide (RGO) with low defects is obtained after 100 seconds of reduction at 2400°C. Through a two-component non-covalent modification, modified reduced graphene oxide (mRGO) is prepared to improve graphene dispersion in the coating while preserving its structural integrity. A graphene/epoxy resin composite radiative heat dissipation coating (GERC) is fabricated using mRGO as the primary filler and aqueous epoxy resin emulsion as the matrix. Additionally, APTES is employed to enhance the adhesion between the coating and the aluminum substrate. By adjusting the filler content, the study investigates the coating's adhesion, thermal conductivity,

radiative heat transfer efficiency, and overall heat dissipation performance to optimize its composition and explore its thermal management mechanism. The results show that the GERC achieves a maximum radiative heat transfer efficiency of 0.93 and an adhesion strength of up to 10.6 MPa. These findings demonstrate the potential of applying GERC on aluminum substrates to enhance the heat dissipation capabilities of spacecraft, providing new insights into the thermal management technology for space radiators.

2 Experimental

2.1 Materials.

The flake graphite (100 mesh) used in the experiments was purchased from Aladdin Reagents Co., Ltd. Hydrogen iodide (HI, 57 wt%) was obtained from Beijing Inokai Technology Co., Ltd. Concentrated sulfuric acid (H_2SO_4, 98 wt%), concentrated hydrochloric acid (HCl, 37 wt%), potassium permanganate ($KMnO_4$, 99 wt%), hydrogen peroxide (H_2O_2, 30 wt%), and ethanol (C_2H_5OH, 99%) were all purchased from Guangzhou Chemical Reagents Factory. 1-Phenyldecanoic acid (PBA) and octylphenol polyoxyethylene ether (POPE) were sourced from Shanghai Macklin Biochemical Technology Co., Ltd. The aqueous epoxy resin emulsion and epoxy resin curing agent (polyamide) were purchased from Shenzhen Jitian Chemical Co., Ltd.

2.2 Preparation of GO, RGO and mRGO

Preparation of graphene oxide (GO) follows an improved method of the Hummers' procedure as outlined by Dong,[19] which yields large-sized GO sheets. The process begins by filtering 2 g of coarse graphite powder through a 100-mesh sieve. The powder is then added to a mixture of 85 mL of concentrated sulfuric acid (H_2SO_4) and 8.5 g of potassium permanganate ($KMnO_4$), and the mixture is allowed to stand for 24 hours. Subsequently, it is transferred to 500 mL of ice water, followed by the addition of 20 mL of hydrogen peroxide (H_2O_2) solution, resulting in the formation of large-sized GO with a yellowish

partially exfoliated appearance. Afterward, 2 mL of a 10:1 hydrochloric acid (HCl) solution is added, and the mixture is dialyzed in a dialysis bag for one week. Finally, a centrifugation step is performed at 3000 rpm to remove any unexfoliated graphite particles from the bottom, yielding a dispersion of large-size GO. The GO dispersion is then freeze-dried to obtain GO powder.

The preparation of reduced graphene oxide (RGO) begins by weighing 0.1 g of GO powder, which is then thoroughly ground in a mortar. The ground powder is sieved through a 100-mesh sieve to select particles with a size smaller than 150 μm. The Joule heat reduction device is shown in Figure S1. The GO powder is uniformly placed in a graphite tube mold with an inner diameter of 5 mm and a length of 5 cm. The mold is positioned between graphite electrodes, and a water-cooled, sealed chamber is mounted and secured. After evacuating the chamber of air, argon gas is introduced to create a reaction atmosphere at 0.1 MPa. The system is then heated to 2400℃ and maintained at this temperature for 100 seconds to facilitate rapid thermal reduction of the GO. After the reaction is complete and the system has cooled, the graphite mold is removed, yielding RGO powder.

The preparation method for non-covalently modified reduced graphene oxide (mRGO) involves placing 0.2 g of RGO powder into a beaker, to which 0.15 g of PBA powder is added. Then, 20 mL of deionized water is introduced into the beaker, and 50 mg of POPE surfactant is gradually added under stirring. The solution is mixed for 2 hours at 1000

rpm, followed by further dispersion in an ultrasonic environment at 40.5 kHz for 12 hours. Finally, the mixture is filtered and dried, yielding mRGO powder.

2.3 Preparation of GERC

First, a silane coupling agent solution is prepared by mixing APTES, deionized water, and anhydrous ethanol in a 1:1:8 ratio. The solution is stirred at 1000 rpm for 1 hour. The aluminum plate, which has been polished and degreased, is then dipped into the silane solution for 5 minutes before being removed. Next, 10 mL of aqueous epoxy resin emulsion is placed in a beaker and treated with ultrasound at 40.5 kHz for 30 minutes to remove air bubbles from the coating matrix. During mechanical stirring at 1000 rpm, 0.2 g of mRGO powder is added. Once the filler is well-mixed, 0.15 g of fumed silica is incorporated, and stirring continues for 1 hour. Subsequently, 5 mL of polyamide epoxy resin hardener is added to the mixture, which is then stirred thoroughly. The mixture is placed in a vacuum drying oven at room temperature for 30 minutes to remove any remaining bubbles, resulting in the GERC. The mass fraction of mRGO in the coating is used to denote the filler content. The amount of fumed silica added to the GERC with different filler contents is consistently 0.15 g.

High-pressure spraying was utilized to coat aluminum plates, with the spray gun connected to an air compressor maintaining stable pressure. For paints of varying compositions and viscosities, air pressure and the spray gun’s material valve were

adjusted to achieve uniform coating. A blank aluminum plate was pre-sprayed to remove residual paint from prior use and confirm unobstructed air and material pathways, enabling timely adjustments to the compressor settings. During formal spraying, aluminum plates were secured on a coating rack, with the spray gun held at a 60–90° angle to the plate surface. Multiple light passes ensured uniform coating, with the number of passes serving as a variable to control coating thickness. Post-spraying, the coating was verified to be free of defects, bubbles, or color inconsistencies, with a smooth surface. The coated plates were air-dried in a dry, ventilated environment at room temperature for over 48 hours, achieving a minimum coating thickness of 20 μm.

2.4 Characterization.

The microstructure of the samples was observed using a cold field emission scanning electron microscope (SEM, Hitachi SU8200) at an accelerating voltage of 10.0 kV. Raman spectroscopy measurements were performed using the H.J.Y. LabRAM Aramis system with a laser wavelength of 532 nm. X-ray photoelectron spectroscopy (XPS) analysis was conducted on the samples using an Axis Ultra DLD system, with Al Kα as the X-ray source for elemental quantification. X-ray diffraction (XRD) analysis was conducted using a D8 Advance (AXS) system, with Cu Kα as the radiation source, a wavelength of 0.15406 nm, a test voltage of 40 kV, and a current of 40 mA for structural characterization. Electrical conductivity measurements were performed using a

DDS-307A conductivity tester (Leici Instruments, Anhui), while the coating emissivity was measured with an IR-2 emissometer developed by the Chinese Academy of Sciences.

3 Results and Discussion

GERC was prepared using the Joule heating method and non-covalent modification of graphene (**Figure 1**). The GO powder appears dark black at the macroscopic level (**Figure 2**a) and shows block-like aggregation under scanning electron microscope (SEM) imaging, with particle sizes ranging from a few micrometers to several tens of micrometers, without distinct layered stacking structures (**Figure 2**d). Due to the strong acid and oxidizing agents used during preparation, GO's surface and edges contain numerous oxygen-containing groups. During the drying process, these polar oxygen groups cause the GO sheets to aggregate, resulting in block-like appearance at the microscopic level. After high-temperature reduction using Joule heating, the GO powder turns gray black (**Figure 2**b) and exhibits a fluffy structure with multi-layered sheet stacking, with sheet diameters ranging from 5 to 10 μm (**Figure 2**e). During the high-temperature reduction process, the oxygen-containing groups in GO are eliminated as gases such as CO_2 and CO, which increases the inter-sheet spacing of the graphene sheets. After non-covalent modification, the reduced graphene oxide (mRGO) retains its sheet size (5–10 μm) (**Figure 2**c), and the multi-layer stacking phenomenon is

significantly reduced, with the graphene sheets distributed more evenly (**Figure 2**f). Non-covalent modification weakens the van der Waals forces between the graphene sheets, reducing the stacking, while the non-covalent modifiers do not chemically react with the graphene, allowing the sheet size to be maintained. The RGO powder, when dispersed in water via ultrasonic treatment, remains briefly dispersed but tends to aggregate due to intermolecular forces and strong hydrophobicity (Figure S2). After 14 days of standing, the RGO and water completely separate, with precipitation occurring (Figure S3). In contrast, mRGO can effectively disperse in aqueous solutions, showing no noticeable precipitation or stratification after 14 days of standing post-ultrasonic dispersion. This demonstrates that non-covalently modified mRGO can remain well-dispersed in aqueous solutions, such as aqueous epoxy resin emulsions, over extended periods. To quantitatively evaluate mRGO dispersion stability in water, we performed Zeta potential measurements. The mRGO exhibited a Zeta potential of approximately -50 mV (Figure S4). This value is significantly below the -30 mV threshold for good colloidal stability. The strong negative potential confirms excellent dispersion stability in aqueous solution. The electrostatic repulsion between particles effectively prevents aggregation and sedimentation over extended periods.

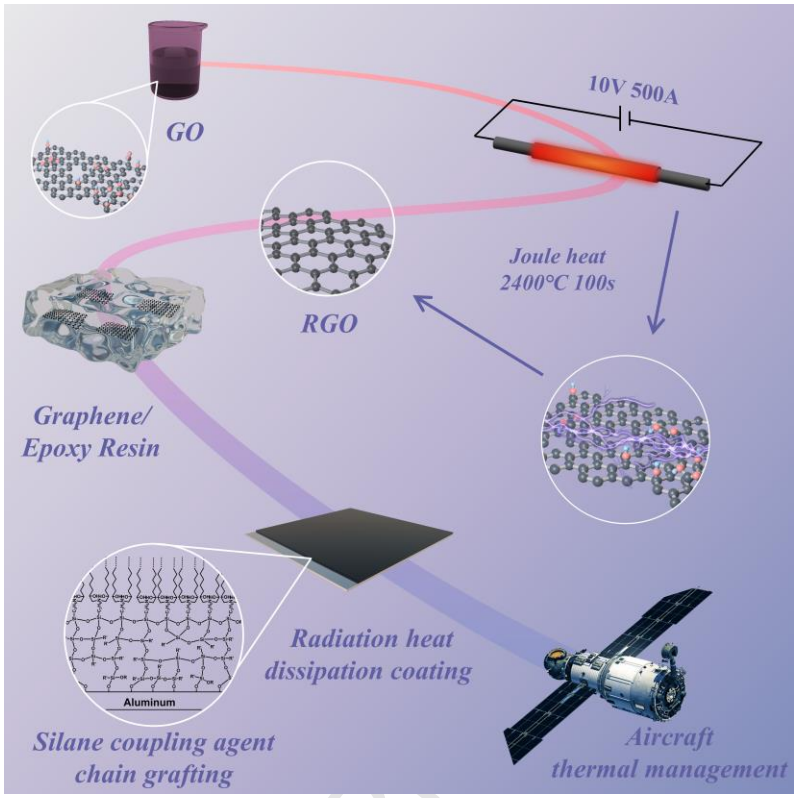

Figure 1. Schematic diagram of the process of preparing GERC.

Raman spectroscopy analysis (**Figure 2**g) revealed that the ID/IG ratio of the GO powder was 1.495, corresponding to a crystallite size of 12.86 nm. For the RGO powder, the ID/IG ratio was 0.124, and the crystallite size increased to 155.037 nm. The ID/IG ratio of the mRGO powder was 0.227, with a crystallite size of 88.690 nm. After rapid high-temperature reduction, most of the oxygen-containing functional groups in GO were removed, resulting in a decrease in defect density and an increase in crystallite size for RGO, which exhibited a more complete crystalline structure. Compared to RGO, the mRGO powder showed an enhanced D-band in the Raman spectrum due to the non-covalent modification. The ID/IG ratio of mRGO increased by 0.103, and the G-band

peak shifted by 3 cm^{-1} to a lower wavenumber. However, the shape of the G-band peak remained largely unchanged, indicating that the PBA molecules attached to the graphene surface through π-π interactions, altering the electron cloud distribution on the surface without significantly affecting the graphene structure. Additionally, both RGO and mRGO exhibited sharp and prominent G-bands in their Raman spectra, indicating that both materials maintained intact lattice structures and high lattice quantization, which suggests that both RGO and mRGO possess excellent thermal radiation properties.

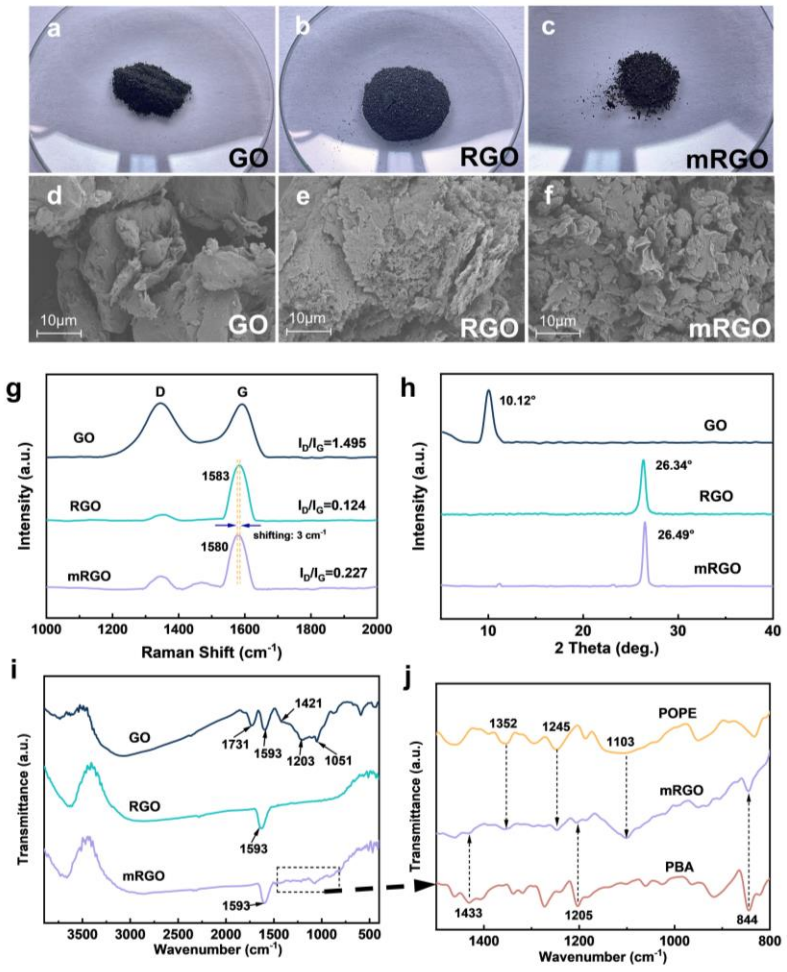

Figure 2. (a)–(c) Photographs of GO, RGO, and mRGO. (d)–(f) SEM images of GO, RGO, and mRGO.

(g) Raman spectra of GO, RGO, and mRGO. (h) XRD patterns of GO, RGO, and mRGO. (i) FTIR spectra of GO, RGO, and mRGO.

From the X-ray diffraction (XRD) results (**Figure 2**h), the diffraction peak of the GO powder appeared at 10.12°, corresponding to a calculated interplanar spacing of 0.873 nm using Bragg's equation. The diffraction peak of the RGO powder shifted to 26.34°, indicating an interplanar spacing of 0.338 nm. For the mRGO powder, the diffraction peak appeared at 26.49°, with an interplanar spacing of 0.336 nm. Compared to RGO, GO contains a significant amount of oxygen-containing groups due to intercalation and oxidation reactions, which create considerable steric hindrance, resulting in an increased interlayer spacing. After rapid high-temperature reduction via Joule heating, most of the oxygen-containing groups in GO were removed, leading to an increase in surface integrity. The van der Waals forces between the graphene sheets caused them to aggregate, reducing the interplanar spacing. The diffraction peak of RGO is located near that of natural graphite at 26.45°, indicating that the prepared RGO material retains a structure similar to graphite with an sp^2 hybridization. After non-covalent modification, the interplanar spacing of mRGO decreased only by 0.002 nm compared to RGO, and the peak shape of mRGO closely resembled that of RGO. This suggests that the non-covalent modification did not cause significant changes to the intrinsic structure of RGO.

Waterborne epoxy resin, a dispersion of epoxy resin in the form of droplets or micelles

in water, retains the excellent adhesion and mechanical properties of conventional epoxy resins while offering lower viscosity and enhanced processability. These characteristics make it widely applicable in industries such as equipment corrosion protection and coatings.[20] The epoxy groups abundant in waterborne epoxy resin emulsions can react with amino groups introduced on aluminum surfaces treated with APTES silane, rendering it an ideal matrix for coatings applied over amino-silane-treated surfaces. The FTIR analysis confirms similar conclusions (**Figure 2**i). Oxygen-containing groups such as carboxyl and epoxy groups appeared on the surface and edges of the sheets under the influence of the oxidizing agent. The peak at 1593 cm^{-1} represents the stretching vibration of the sp^2 hybridized C=C bonds in graphene. After rapid high-temperature reduction, the RGO powder shows almost no peaks between 1500 and 800 cm^{-1} that correspond to oxygen-containing functional groups. However, the C=C vibration peak at 1593 cm^{-1}, representing the sp^2 hybridized structure of graphene, is retained. This suggests that the rapid high-temperature reduction effectively removed oxygen-containing functional groups on the surface of GO while preserving the sp^2 hybridized structure of graphene. After non-covalent modification, the mRGO powder retains the C=C double bonds of graphene, and multiple new functional groups reappear in the 1500–800 cm^{-1} range. The peaks at 1352 cm^{-1} and 1245 cm^{-1} correspond to hydroxyl groups, and the peak at 1103 cm^{-1} represents ether groups from the POPE molecules, while the peaks at 1205 cm^{-1} and 1433 cm^{-1} are assigned to the C=O

stretching vibration of carboxyl groups, and the peak at 844 cm^{-1} is attributed to C-H vibrations from the PBA molecules. These hydrophilic groups, which are introduced into the graphene structure through non-covalent modification, effectively enhance the dispersion of mRGO in water (**Figure 2**j). This indicates that non-covalent modification of graphene with POPE and PBA introduces hydrophilic groups such as ether and carboxyl groups, without disrupting the sp^2 hybridized structure of the graphene.

To enhance the adhesion of the coating to the aluminum substrate, the construction of a silane grafting network using APTES is an effective strategy (**Figure 3**a). APTES forms a silane network on the aluminum surface through hydrolysis and condensation processes, where silanol groups (Si-OH) play a key role in interacting with the aluminum substrate to improve adhesion. During the hydrolysis and condensation processes, the generation and consumption of Si-OH groups affect the conductivity of the solution, while intermolecular condensation leading to the formation of Si-O-Si bonds is crucial for the polymerization of silane molecules into chain-like structures in the solution.

The silane grafted surface treatment layer has a thickness of approximately 3 to 5 μm, with a dense and uniform distribution on the aluminum plate surface (**Figure 3**b). During the hydrolysis of APTES solutions with varying concentrations, the conductivity of the solution initially increases, then decreases, and finally stabilizes (**Figure 3**c). Initially, the hydrolysis of the silane generates Si-OH, increasing the ion concentration in the solution and raising the conductivity. As the Si-OH groups condense and are consumed, the rate of

conductivity increase slows down until a maximum value is reached. Afterward, the rate of Si-OH formation slows, and the conductivity decreases until it stabilizes, indicating the continuous formation of Si-O-Si bonds. FTIR analysis shows that after 1 hour of hydrolysis, the Si-OH group content in silane solutions with different compositions increases with the amount of silane (**Figure 3**d). When the silane content is low, the Si-OH generated through hydrolysis condenses to form Si-O-Si bonds, resulting in a lower Si-OH content. As the silane content increases to 10-20%, the Si-OH content rises, but after exceeding 10%, further increases in silane concentration do not significantly enhance the grafting reaction. This is due to elevated water content accelerating silane condensation reactions. The condensation process, driven solely by silanol groups, depends on their concentration in the solution. Water content regulates silanol concentration by influencing the hydrolysis rate of silanes. At a fixed silane concentration, higher water content increases silanol concentration, thereby enhancing the condensation reaction rate. Therefore, a silane content of 10% is optimal, as it maintains a high Si-OH content while allowing an appropriate amount of Si-O-Si groups to participate in the formation of the silane layer. Therefore, a silane content of 10% is optimal, as it maintains a high Si-OH content while allowing an appropriate amount of Si-O-Si groups to participate in the formation of the silane layer. The adhesion strength between GERC and Al substrate without APTES modification was measured to be 3.0 MPa. After silane surface treatment, the adhesion strength of the coating on the aluminum plate

significantly increases by an average of 273% (Figure 3e). The adhesion strength of the silane grafted coating on the aluminum plate is maximized at 10.2 MPa, which is 3.4 times higher than that of the untreated aluminum plate. Both silane and water content initially increase, then decrease, with the optimal adhesion occurring at 10% silane content and 10% deionized water content. The silane grafting surface treatment can enhance the density of the silane treatment layer and improve coating adhesion by introducing amino groups while maintaining the level of silane molecular grafting.

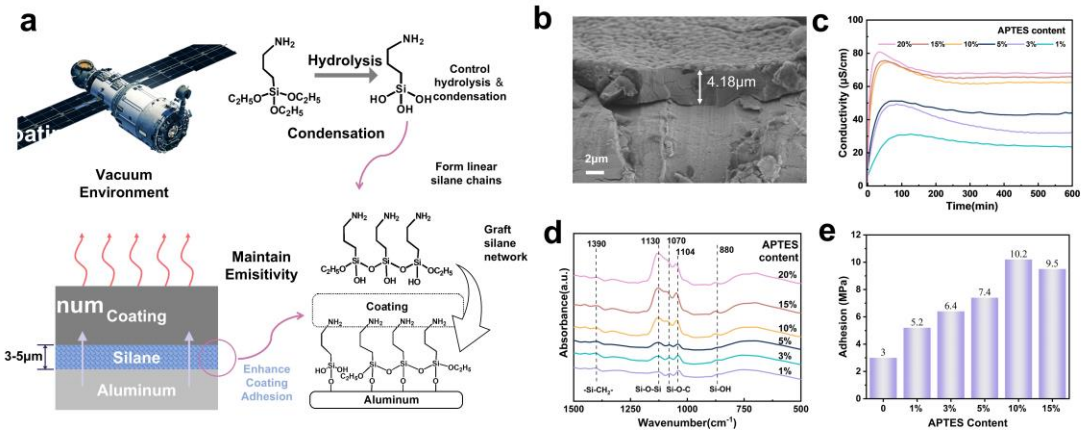

Figure 3. (a) Schematic diagram of the reaction between GERC and APTES; (b) SEM image of APTES on the aluminum surface; (c) Variation of the hydrolysis conductivity of APTES solutions with different concentrations over time; (d) FTIR spectra of solutions with different APTES concentrations after 1 hour of hydrolysis; (e) Adhesion strength tests of GERC with different APTES concentrations.

The scanning electron microscopy (SEM) and Mapping results show that the elements carbon (C), nitrogen (N), oxygen (O), and silicon (Si) are evenly distributed on the surface of the coating, with no aggregation observed, indicating that the mRGO filler

and the silica are well-dispersed within the coating (**Figure 4**a).The elemental mapping analysis shows that all constituent elements are uniformly distributed across the coating surface without significant aggregation, suggesting that both mRGO and fumed silica fillers are well dispersed within the coating matrix(Figure 4b). Mapping analysis further confirms that, aside from carbon, which is concentrated at the graphene locations, other elements are uniformly distributed throughout the coating. Cross-sectional SEM images of the composite radiation heat dissipation coating clearly show the layered structure consisting of the aluminum plate, silane treatment layer, and graphene radiation heat dissipation coating. The reaction between the silane and the aluminum surface forms a dense silane treatment layer, enhancing the adhesion between the coating and the aluminum plate (**Figure 4**c). XRD analysis revealed characteristic diffraction peaks for each component. The diffraction patter of the composite coating showed peaks corresponding precisely to those of individual components, confirming the reliability of the coating composition analysis. Thermogravimetric (TG) analysis of the coating shows a slight decrease in mass in the low-temperature range due to the evaporation of bound water(**Figure 4**e), a rapid decrease between 200 and 400°C due to the thermal decomposition of the epoxy resin matrix, and a continued reduction after 400°C due to the decomposition of the graphene modification agent, demonstrating excellent thermal stability. The surface of the GERC composite radiation heat dissipation coating on the aluminum plate is smooth and free of spraying defects, exhibiting a matte black

appearance (**Figure 4**h). The crosshatch adhesion test demonstrates excellent adhesion of the coating (**Figure 4**i). Cross-sectional SEM images again confirm the layered structure of the aluminum plate, silane treatment layer, and graphene radiation heat dissipation coating, with the silane reacting with the aluminum surface to form a dense silane treatment layer, thus enhancing the adhesion between the coating and the aluminum plate.

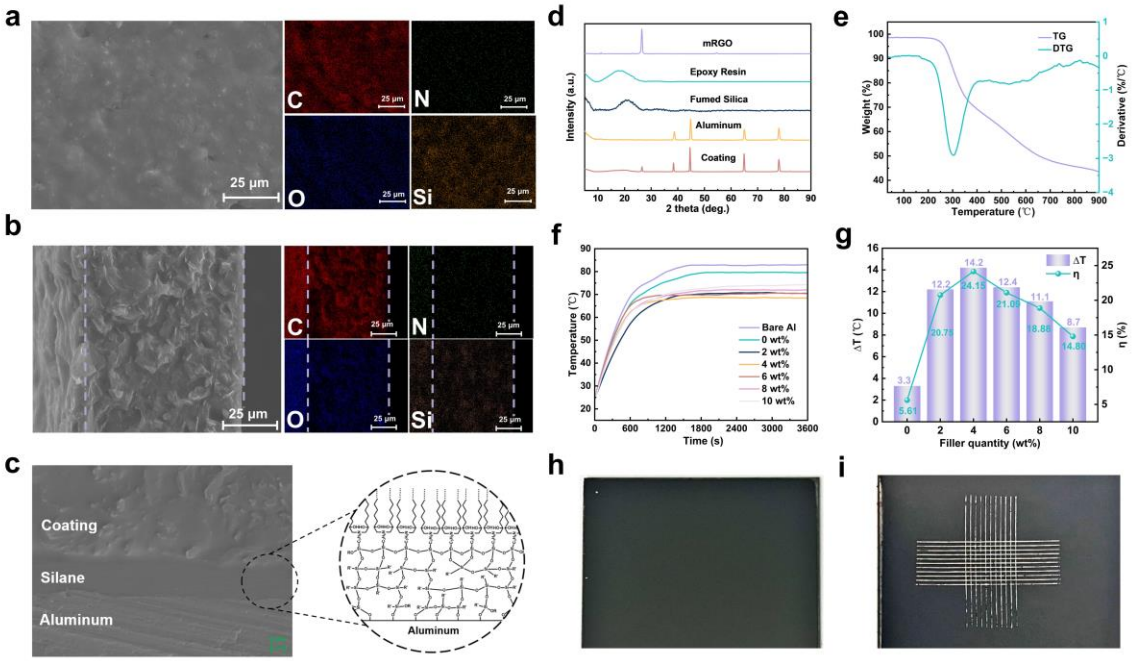

Figure 4. (a) SEM image of the surface of GERC and EDS elemental analysis for C, O, N, and Si. (b) SEM image of the cross-section of GERC and EDS elemental analysis for C, O, N, and Si. (c) SEM image of the cross-section of GERC and the interface bonding mechanism of GERC. (d) XRD patterns of GERC and its constituent materials. (e) TG and DTG curves of GERC. (f) Temperature rise curves of GERC with different mRGO filler contents. (g) Thermal gradient (ΔT) and thermal efficiency (η) of GERC with different mRGO filler contents. (h) Surface morphology of GERC. (i) Schematic diagram of the grid

method for adhesion testing of GERC.

GERC were applied to the surface of silane-treated aluminum substrates using a spray coating method. The experimental setup for testing the heat dissipation efficiency of the coating is shown in Figure S5. The experimental results (**Figure 4**f) indicated that the blank aluminum substrate, which had not been coated with the GERC, reached a final equilibrium temperature of 82.8°C under a heating power of 6 W. The equilibrium temperature of the GERC with added mRGO filler decreased by 3.3°C compared to the blank aluminum substrate. When the mRGO filler content reached 4 wt%, the equilibrium temperature was minimized at 68.6°C, with the highest heat dissipation efficiency of 24.15% (**Figure 4**g). Under identical testing conditions with a 3 wt% content, the mRGO coating exhibited a heat dissipation efficiency 37.4% higher than that of GO and 15.2% higher than that of RGO. These findings indicate that modifying RGO into mRGO significantly enhances its radiative and thermal performance. This improvement is attributed to the formation of a network-like thermal conductive pathway due to the increased mRGO content, which facilitates heat transfer to the surface of the coating and promotes infrared photon radiation. However, further increases in mRGO filler content led to a decrease in the surface emissivity of the coating, thereby reducing the heat dissipation efficiency. Additionally, an increase in filler content also caused a reduction in the coating's adhesion. Therefore, considering both heat dissipation performance and adhesion, the optimal mRGO filler content is 4 wt%.

Blank aluminum plate surface emissivity of 0.35, while the emissivity of the epoxy resin-coated aluminum substrate with 0 wt% filler increased to 0.64. The application of the GERC was shown to enhance the emissivity of the aluminum substrate under various filler contents and coating thickness conditions. Specifically, as the amount of micron-sized reduced graphene oxide (mRGO) filler increased, the coating emissivity initially stabilized and then decreased. Beyond this point, the emissivity gradually decreased with further increases in filler content. The emissivity reached its peak value of 0.93 at 2 wt% and 4 wt% mRGO filler content. The emissivity and thermal performance of GO, RGO and mRGO coatings at 3 wt% concentration was also compared. The results show that mRGO exhibits superior performance compared to GO and RGO due to its stronger structural integrity and higher thermal conductivity. mRGO achieves an emissivity of 0.93, which is significantly higher than GO (0.85) and RGO (0.88). Additionally, the increase in coating thickness had little effect on the surface emissivity of the composite radiation heat dissipation coating. Given the uniform distribution of filler within the coating and the absence of significant defects during the formation process, the increase in coating thickness did not alter the surface structure or lattice characteristics of the coating, thus having no significant impact on its emissivity.

Within the GERC, the random distribution of graphene flakes forms a complex thermal conduction network (**Figure 5**a). Due to the inherent superior in-plane thermal conductivity of graphene, this random arrangement of graphene flakes enhances the

thermal conductivity of the epoxy resin in all directions, thereby increasing its thermal conductivity. As the filler content increases, the spacing between the graphene flakes decreases, leading to a corresponding increase in the overall thermal conductivity of the GERC. The high surface roughness of the GERC can be attributed to its numerous microscopic protrusions and indentations. These microstructures cause the incident thermal radiation to undergo multiple absorption and reflection events on the surface, reducing the energy of reflected radiation and thereby increasing the GERC's absorption rate. When electromagnetic waves penetrate the GERC, infrared radiation experiences multiple absorption processes within the multilayer graphene flakes, reducing the infrared transmittance of the graphene layers and further enhancing the absorption rate. Moreover, due to the random distribution of graphene within the GERC, thermal radiation also undergoes multiple reflections and absorptions between the graphene flakes, forming a "miniature blackbody" structure (**Figure 5**b), which imparts exceptional infrared absorption properties to the GERC. From the perspective of infrared radiation (**Figure 5**c), the presence of graphene materials with a highly quantized lattice structure within the GERC allows efficient conversion of heat into thermal radiation due to lattice vibrations upon thermal excitation, which is subsequently radiated into the surrounding environment. The combined effects of these factors contribute to the high infrared emissivity of the composite GERC. GERC is particularly suitable for thermal management systems in spacecraft. It can be applied to external surfaces, such as

radiators, to enhance heat dissipation while minimizing solar heat absorption. Additionally, its lightweight and durable properties make it ideal for use in harsh space environments.

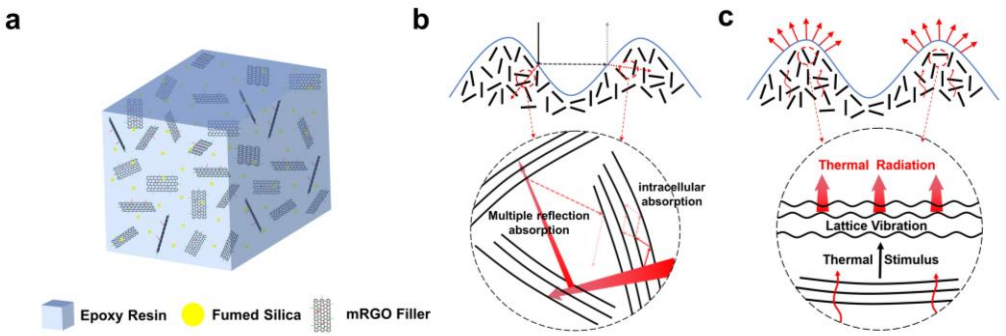

Figure 5. (a) Schematic diagram of the internal structure of the GERC; (b) Schematic diagram of infrared radiation absorption by the GERC; (c) Schematic diagram of infrared radiation emission from the GERC

4 Conclusions

This study successfully developed a graphene/epoxy composite radiation heat dissipation coating. Low-defect graphene was prepared via rapid Joule heating reduction, and its uniform dispersion in aqueous epoxy resin was achieved through non-covalent modification. Experimental results show that the coating, with a filler content of 4 wt% modified reduced graphene oxide, exhibits excellent heat dissipation performance and adhesion strength, with an emissivity of 0.93 and an adhesion strength of 10.6 MPa. By enhancing the surface emissivity and thermal conductivity of the aluminum substrate, the coating significantly improves the heat dissipation efficiency of spacecraft. These

findings provide new material options and technical solutions for spacecraft thermal management, offering broad application potential.

ASSOCIATED CONTENT

Supporting Information

Schematic diagram of high-temperature rapid reduction device (Figure S1). RGO and mRGO powders were sonicated in water and left to stand for 1 min (Figure S2). RGO and mRGO powders were sonicated in water and then left to stand for 14 days (Figure S3)

AUTHOR INFORMATION

Corresponding Author

Jing Li−School of Chemistry and Chemical Engineering, South China University of Technology, Guangzhou 510641, China; South China University of Technology-Zhuhai Institute of Modern Industrial Innovation, Zhuhai 519000, P. R. China; Email: ljing@scut.edu.cn

Yawei Xu -- National Key Laboratory of Spacecraft Thermal Control, Beijing Institute of Spacecraft System Engineering, Beijing 100086, P. R. China;

18792530289@163.com

Authors

Ning Li -- School of Chemistry and Chemical Engineering, South China University of Technology, Guangzhou 510641, P. R. China;

https://orcid.org/0009-0002-0642-2469; Email: celining@mail.scut.edu.cn

Zhang Yibo-- School of Chemistry and Chemical Engineering, South China University of Technology, Guangzhou 510641, P. R. China.

Notes

The authors declare no competing financial interest.

ACKNOWLEDGEMENT

This work was supported by the Shanghai Aerospace Science and Technology Innovation Foundation (SAST2022-047).

References

[1] Abbas A, Wang C C. Augmentation of natural convection heat sink via using displacement design. International Journal of Heat and Mass Transfer, 2020, 154: 119757.

[2] Gong X, Qian R J, Xue H Y, et al. Progress of microscopic thermoelectric effects studied by micro- and nano-thermometric techniques. Frontiers of Physics, 2022, 17(2): 23201.

[3] Kianfar, K.; Joodaki, S.; Dashti, I.; Asghari, S. Lifetime estimation of heat pipes in space applications using particle filtering, Arrhenius and FIDES methods. Therm. Sci. Eng. Prog. 2021, 22, 100847.

[4] Nobrega G, Cardoso B, Souza R, et al. A review of novel heat transfer materials and fluids for aerospace applications. Aerospace, 2024, 11(4): 275.

[5] Butler A, Argyropoulos C. Mechanically tunable radiative cooling for adaptive thermal control. Applied Thermal Engineering, 2022, 211: 118527.

[6] Chu W X, Lin Y C, Chen C Y, et al. Experimental and numerical study on the performance of passive heat sink having alternating layout. International Journal of Heat and Mass Transfer, 2019, 135: 822-836.

[7] Zhang S Y, Li Y, Yang H, et al. Multifunctional Superhydrophobic Composite Coatings with Remarkable Passive Heat Dissipation and Anticorrosion Properties. Industrial & Engineering Chemistry Research, 2021, 60(30): 11019-11029.

[8] Kung F, Yang M C. Improvement of the heat-dissipating performance of powder coating with graphene. Polymers, 2020, 12(6): 1321.

[9] Hadi A M, Ismael M A, Alhattab H A. Experimental investigation of thermal performance of the graphene-coated Al heat sink [J]. Materials Today: Proceedings, 2021, 42: 2779-2784.

[10] Zu H Y, Dai W, Li Y, et al. Analysis of enhanced heat transfer on a passive heat sink with high-emissivity coating [J]. International Journal of Thermal Sciences, 2021, 166: 106971.

[11] Lee J, Kyeong D, Kim J, et al. Layer-by-layer self-assembled functional coatings of carbon nanotube-polyethylenimine for enhanced heat transfer of heat sinks[J]. International Journal of Heat and Mass Transfer, 2022, 184: 122344.

[12] He J, Wang H, Qu Q Q, et al. Three-dimensional network constructed by vertically oriented multilayer graphene and SiC nanowires for improving thermal conductivity and operating safety of epoxy composites with ultralow loading. Composites Part A: Applied Science and Manufacturing, 2020, 139: 106062.

[13] Guo X M, Feng S W, Yi P, et al. Heat dissipation performance of graphene anti-corrosive coatings for high-heat flow equipment. Journal of Physics: Conference Series, 2023, 2524(1): 012034.

[14] Teng T P, Chen W J, Chang C H. Enhanced heat dissipation performance of automotive led lamps using graphene coatings. Polymers, 2021, 14(1): 50.

[15] Cheng C, Shi W H, Teng T P, et al. Evaluation of surfactants on graphene dispersion and thermal performance for heat dissipation coating. Polymers, 2022, 14(5): 952.

[16] Liang P Y, Wang W, Xin J J, et al. In situ combustion synthesis of Gr/h-BN composites and its passive heat dissipation application. ACS Omega, 2022, 7(41): 36786-36794.

[17] B. Wang, X. Li, Z. Hu, S. Wang, W. Dong, B. Wang, L. Wang, N. Gong, Functionalization of aluminum alloy surface with reactive epoxide silane to induce ultra-high strength polyamide 6 / aluminum alloy composite joint, Appl. Surf. Sci. (2023) 626, 157231.

[18] S.R. Lee, K. Man Bae, J.J. Baek, M.C. Kang, T.I. Lee, Adhesion enhancement between aluminum and butyl rubber by (3-mercaptopropyl) trimethoxy silane for vibration damping plate, J. Adhes. Sci. Technol. (2021) 35(10), 1114-1124. doi:10.1080/01694243.2020.1837564.

[19] Dong, L.; Chen, Z.; Lin, S.; Wang, K.; Ma, C.; Lu, H. Reactivity-Controlled Preparation of Ultralarge Graphene Oxide by Chemical Expansion of Graphite. Chemistry of Materials 2017, 29 (2), 564–572.

[20] Ai D, Mo R, Wang H, et al. Preparation of waterborne epoxy dispersion and its application in 2K waterborne epoxy coatings. Progress in Organic Coatings, 2019, 136: 105258.

Declaration of interests

☒ The authors declare that they have no known competing financial interests or personal relationships that could have appeared to influence the work reported in this paper.

☐ The authors declare the following financial interests/personal relationships which may be considered as potential competing interests:

Highlights

1. Joule heating was utilized for rapid (100 s) reduction of graphene oxide to low-defect graphene.

2. A graphene/epoxy composite coating achieved high infrared emissivity (0.93).

3. This work provides a novel solution for spacecraft thermal management by enhancing the thermal efficiency of aluminium alloy heat sinks in spacecraft.